ZOOLOGICAL SCIENCE 17: 911–933 (2000)

Morphological Characteristics of the Developing Cranial Nerves and Mesodermal Head Cavities in Sturgeon Embryos from Early Pharyngula to Late Larval Stages

Shigeru Kuratani*, Yoshiaki Nobusada, Hajime Saito and Yasuyo Shigetani

Department of Biology, Faculty of Science, Okayama University 3-1-1 Tsushimanaka, Okayama 700-8530, Japan

ABSTRACT—As sturgeons are considered to represent a basal group of Osteichthyes, it is necessary to evaluate their developmental features to understand the evolution, not only of bony fishes, but also of tetrapods in general. Using Besters, commercially established hybrid sturgeons, the neural crest cell distribution pattern, mesodermal epithelium, and peripheral nerves were observed based on whole-mount immunostained and -sectioned embryos, from the pre-hatching embryonic stage to a late swimming larval stage. At the early pharyngula stage, the hindbrain exhibits at least six rhombomeres. These have a typical arrangement of neuroepithelial cells, and segmentally distributed cephalic crest cell populations associated with even-numbered rhombomeres medially, and single pharyngeal arches laterally. The head cavities first arise as a pair of epithelial primordia in the prechordal region. Secondarily, the cavity is subdivided mediolaterally into the premandibular and mandibular cavities. These mesodermal components never affect the segmental pattern of cranial nerve roots as seen in the shark embryo (Kuratani and Horigome, 2000), probably due to the early degeneration of the cavities. The hyoid cavity never appears. As observed in several teleosts, the newly hatched Bester larva possesses extensive neurites in the epidermis, originating from both trigeminal placodes and Rohon-Beard cells. This neurite network diminishes during development, in concordance with the appearance of lateral line nerves. All the epibranchial placodes are seen as focal, HNK-1-positive epidermal thickenings and give rise to inferior ganglia of the branchiomeric nerves. Metameric morphology of the branchiomeric nerve innervation is secondarily disturbed through modification of the head region, involving the expansion of the operculum and modification of the jaw.

INTRODUCTION

Sturgeons are generally regarded as one of the most primitive groups among Osteichthyes since a large part of their endoskeleton remains cartilaginous and several anatomical features resemble those of sharks. However, their Paleozoic ancestors are now known to have possessed highly ossified skeletal systems. As a sister group of polypterids, sturgeons have been classified in Chondrostei until recently. They are now considered to belong to the group Acipenseriformes, together with paddle fish, gars, and *Amia* (bowfin) (Grande and Bemis, 1996), although their phylogenetic position still remains enigmatic (see Bond, 1996; and references therein). Nevertheless, sturgeons and those fish that belong to the Holostei (gars and *Amia*; Romer and Parsons, 1977) possess a number of features that are absent from teleosts. Along with the uneven holoblastic cleavage, not discoidal as in teleosts, the embryos exhibit an expanded head region over the yolk at early pharyngular stage, reminiscent of amphibian development (Balfour and Parker, 1882; Dean, 1895; Eycleshymer and Wilson, 1906). Their early larvae also resemble those of amphibians (Kerr, 1900, 1901; reviewed by Keibel, 1906). Lungfish share these apparently primitive features. Acipenseriformes and teleosts also share a similar mode of gastrulation (Keibel, 1906). Sturgeons thus represent an important group of animals in the understanding of the embryogenetic changes that took place in the evolution of Osteichthyes as well as of tetrapods.

Except for the developmental stages (Bolker, 1993), the embryonic development of sturgeons has been less extensively studied than for Chondrichthyes. In the latter group, pharyngula embryos were previously believed to exhibit a typical vertebrate body plan. This judgment was based on the possession of head cavities (segmented head mesoderm), and well-segmented peripheral nerve primordia, including neural crest cell populations and epibranchial placodes that are associated with the metameric pattern of pharyngeal arches (Balfour, 1878; van Wijhe, 1882; Kupffer, 1891; Goodrich, 1930; Batten, 1957a, b; Bjerring, 1977; reviewed

* Corresponding author: Tel. +81-86-251-7867;
FAX. +81-86-251-7876.
E-mail. sasuke@cc.okayama-u.ac.jp

by Jarvik, 1980). In particular, the presence of segmented mesoderm, or head cavities, was previously compared with the segmentation of somites in the trunk, and these epithelial mesodermal regions maintain a close relationship with peripheral nerve distribution in the shark embryo (Kuratani and Horigome, 2000). The head cavities become less distinct in amniotes, although epithelial mesodermal cysts do develop in many species at late stages of pharyngula. Instead, amniotes exhibit incomplete segmentation in head mesoderm that does not seem to have any relationship with peripheral nerve patterning (reviewed by Kuratani, 1997). Thus, the evolutionary transition of mesodermal development remains unclear. Although primitive bony fish, including sturgeons, also exhibit head cavities (Ostroumow, 1906; de Beer, 1924; reviewed by Brachet, 1935; and by Jacob *et al.*, 1984), their developmental sequence and topographical relationships have not been reported.

The problem of vertebrate head segmentation is becoming a serious topic of developmental biology, in which cellular and molecular aspects of morphogenesis are analyzed. Compartmentalized segments are present in the developing brain as neuromeres, being established through restriction of neuroepithelial cell lineages (Fraser *et al.*, 1990), and segmentally regulated gene expression. These features are also shared by neural crest cell populations and the mesenchyme derived from the neurectoderm, clearly showing the presence of a metameric developmental program in the head of vertebrate embryos (Lumsden and Keynes, 1989; Figdor and Stern, 1993; reviewed by Kuratani, 1997; and by Kuratani *et al.*, 1999). Among such developmental compartments, rhombomeres are the segments in the hindbrain, and two successive segments correspond to a single pharyngeal arch by means of branchiomeric nerves (reviewed by Lumsden and Keynes, 1989).

It is necessary to evaluate the embryonic morphology of Osteichthyes, not only to understand the vertebrate body plan, but also to trace the changes of morphogenetic processes in evolution. For that purpose, sturgeons are very suitable for comparative and evolutionary studies. Here, we used the Bester, a commercially established hybrid between *Acipenser ruthenus* and *Huso huso* (beluga), maintained artificially fertilized eggs, and obtained a series of developing embryos. Based on histological and whole-mount specimens, we found that the rhombomeres and cranial nerve morphology of the Bester are well conserved, but that the developmental sequence of the head mesoderm is apparently modified as compared with other vertebrates.

MATERIALS AND METHODS

Whole-mount immunostaining

Fertilized Bester eggs (a gift from Tsukuba Research Institute, Fujikin Inc. Ltd., Tsukuba, Japan) were brought into the laboratory and kept in fresh water at 16–17°C. Embryonic stages were determined according to body length and morphological features that were consistent with the post-oviposition age (Table 1). To observe the peripheral nerve morphology in developing Bester embryos and larvae, we tested several different monoclonal antibodies that had been shown to recognize neurons. Of these, HNK-1 (Leu-7, Becton Dickinson, San Jose, CA) was the most suitable for this purpose. To obtain stability of the carbohydrate epitope as well as permeability of the antibody, embryos and larvae were fixed with Bouin's fixative at 4°C for 1 day. The embryos were washed and dehydrated in a graded series of ethanol (70%, 95%) and stored at 4°C. They were placed in Dent's fixative, a mixture of dimethyl sulfoxide (DMSO) and methanol (1:4) for several days for de-pigmentation and blocking of endogenous peroxidase activities. Half a ml of 10% Triton X-100/distilled water was added and the embryos were further incubated for 30 min at room temperature. After washing in Tris-HCl-buffered saline[OLE4] (TST: 20 mM Tris-HCl, pH 8.0, 150 mM NaCl, 0.01% Triton X-100), the samples were blocked with 5% non-fat dried milk in TST (TSTM). The embryos were incubated in the primary antibody (HNK-1, diluted 1/100 in spin-clarified TSTM containing 0.1% sodium azide) for 2 to 4 days at room temperature while being gently agitated on a shaking platform. The secondary antibody used was horseradish peroxidase (HRP)-conjugated goat anti-mouse IgM (ZYMED Lab. Inc., San Francisco, CA) diluted 1/200 in TSTM. After final washing in TST, the embryos were preincubated with peroxidase substrates 3,3'-diaminobenzidine (DAB: 100 μg/ml) in TS for 1 hr. They were allowed to react in Tris-HCl-buffered saline at the same concentration of DAB with 0.01% (v/v) hydrogen peroxide (35% aqueous solution) for 20 to 40 min at 0°C. The reaction was stopped, and the embryos were placed in 0.5% KOH. The latter treatment successfully cleared the soft tissue of the embryos (Fig. 1). The stained embryos were then transferred to a graded series of glycerol/water solutions, and stored in 60% glycerol in water for observation.

Table 1. Developmental stages of bester

specimen	body length (mm)	post-oviposition age (days)	stages
404N2	–	2	x
40424P	–	2.5	y
4056P	–	3	z
418	–	3	A
418–1140	–	3	A
419–1235	6.5	4	B
420–1330	9.0	5	C
421–1200	10.0	6	D
421–2145	11.0	6	D
422–2210	11.0	7	E
423	11.0	8	E
425–2300	14.5	10	F
429–1420	19.5	14	G

For staining of the muscle tissue, MF-20 antibody (purchased from the Developmental Studies Hybridoma Bank, Iowa City, Iowa) was used for the primary antibody. In this case, embryos were fixed with 4% paraformaldehyde in 0.1% phosphate-buffered saline at 4°C for 1 day.

Immunostaining of sectioned specimens

Specimens fixed with Bouin's fixative were embedded in paraffin and sectioned at 7 μm. They were deparaffinized and treated with 1% periodic acid for 5 min at room temperature, followed by washing in TST. The monoclonal antibody, HNK-1, was used to label the developing nervous system on the sectioned specimens. The primary antibody were diluted in TSTM and applied to the sections for 1.5 hr at room temperature. After washing with TST, secondary antibodies, HRP-anti mouse IgM (ZYMED Lab. Inc.), were diluted 1/200 in TSTM and applied to the specimens for 40 min. The sections were counter-

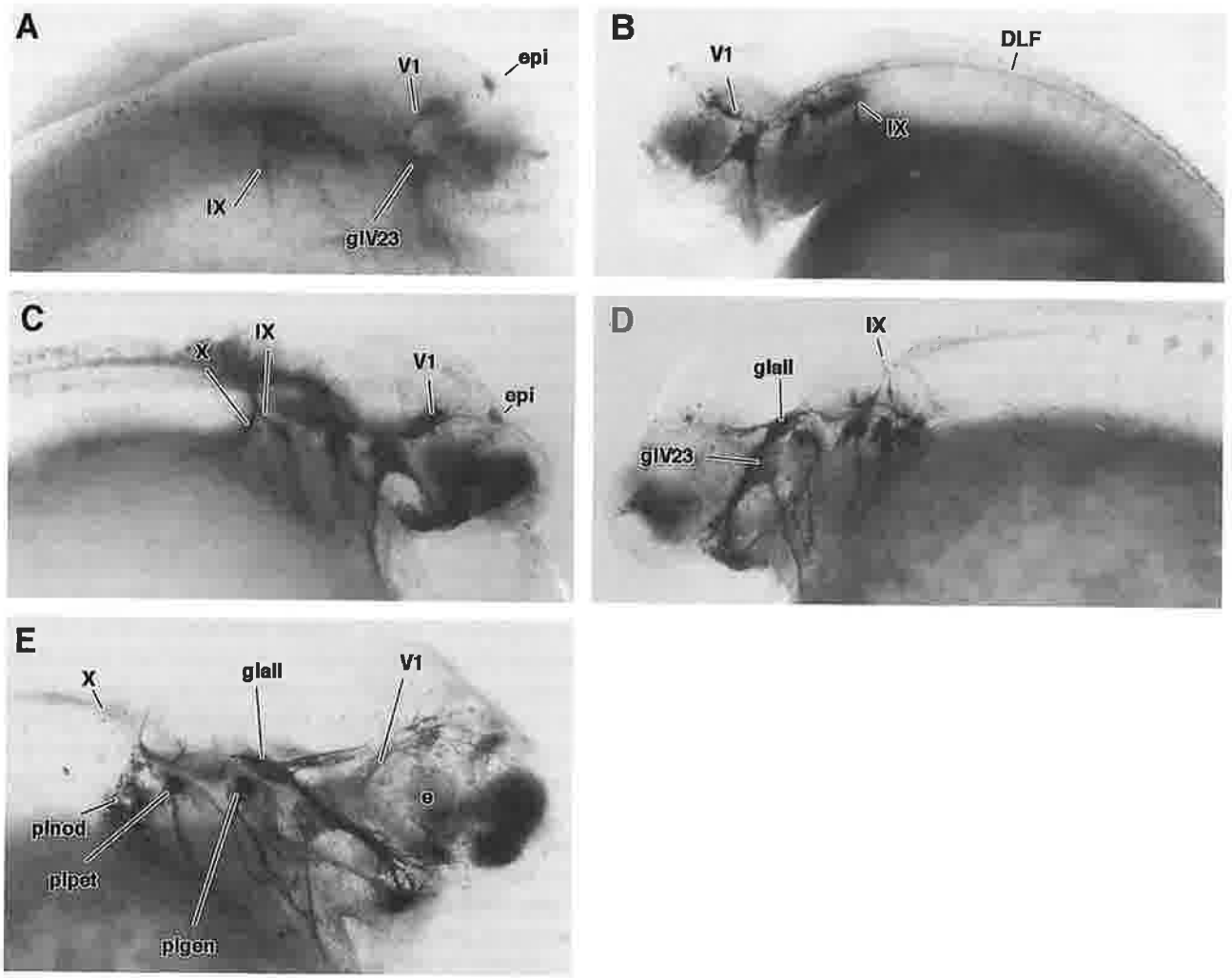

Fig. 1. Whole-mount Bester embryos and larvae immunochemically stained with HNK-1 antibody and treated with 0.5% KOH. Lateral views. Stages A (A) to E (E) are shown. For similarly treated embryos at stage F, see Fig. 10C. Only part of the neural structures are labeled. For detailed descriptions and scales, see the following line drawings.

stained either with cresyl violet or hematoxylin after the peroxidase reaction.

Abbreviations

ac	anterior commissure
all	anterior lateral line nerve
ao1	aortic arch 1
ba	barbel or its primordium
BC	branchial crest cells
com	communicating branch of the lateral nerves
cp	posterior commissure
da	dorsal aorta
di	diencephalon
dlf	dorsolateral fasciculus
drg	dorsal root ganglion
e	eye
epi	epiphysis
exg	external gills
exn	external nares
fb	forebrain
fp	frontal process (=Haftorgan of von Kupffer, 1906)
glgn	geniculate ganglion of the facial nerve
glall	anterior lateral line nerve ganglion
glmid	middle lateral line nerve ganglion
glpll	posterior lateral line nerve ganglion
glpt	petrosal ganglion of the glossopharyngeal nerve
gV23	trigeminal ganglion
h	heart
hb	hindbrain
hc	head cavity
HC	hyoid crest cells
hm	hyomandibular ramus of the facial nerve
hyc	hyoid cavity of the shark embryo
hyp	hypophysis
hypt	hypothalamus
II	optic nerve
III	oculomotor nerve
IV	trochlear nerve
IX	glossopharyngeal nerve or its anlage
mb	midbrain
mid	middle lateral line nerve
mlf	medial longitudinal fasciculus
mm	mandibular arch muscle plate
mmp	maxillomandibular prominence
mn	mandibular process
mnd	mandibular mesoderm in the lamprey

mnc	mandibular cavity
mx	maxillary process
myo	myotomes
nolf	olfactory nerve
nt	notochord
olep	olfactory epithelium
op	operculum
opm	oropharyngeal membrane
ot	otocyst
ov	optic vesicle
pa2–3	pharyngeal arches 2 to 3
pf	pectoral fin
phr	pharynx
plgen	geniculate placode
plnod	nodose placode
ploph	ophthalmic placode
plpet	petrosal placode
pltrg	trigeminal placode
poc	postoptic commissure
pog	preoral gut
pp1–3	pharyngeal pouches 1 to 3
prc	pericardium
prcm	prechordal mesenchyme
prmc	premandibular cavity
prnd	pronephric duct
r1–6	rhombomeres 1 to 6
rb	buccal branch of the anterior lateral line nerve
RB	Rohon-Beard cells
rop	opercular ramus of the facial nerve
rophs	superficial ophthalmic branch of the anterior lateral line nerve
rpd	dorsal pharyngeal branch of the glossopharyngeal nerve
rpl	palatine branch of the facial nerve
rpll	posterior branch of the posterior lateral line nerve
rprIX	pretrematic branch of the glossopharyngeal nerve
rptIX	posttrematic branch of the glossopharyngeal nerve
rptVII	posttrematic branch of the facial nerve
rptX1	posttrematic branch of n. X1
rr	rostral (or maxillary) branch of the trigeminal nerve
rv	ventral (or mandibular) branch of the trigeminal nerve
soc	tract of supraoptic commissure
som	somites
spt	supratemporal branch of the posterior lateral line nerve
tel	telencephalon
thc	tract of habenular commissure
tpoc	tract of postoptic commissure
V	trigeminal nerve or its primordium
V1	profundal nerve or its primordium
V23	trigeminal nerve
v4	fourth ventricle
VII	facial nerve
VIII	acoustic nerve
X	vagus nerve

RESULTS

Stage A

The youngest Bester embryo observed in the present study corresponded to an early pharyngula (Fig. 2). The brain at this stage resembled that seen in 70-hr embryos of *Acipenser sturio* by von Kupffer (1906; Fig. 3A). The processus neuroporicus protruded at the site of the closure of the neural pore, and a parencephalic prominence (von Kupffer, 1906), or saccus dorsalis (Nieuwenhuys, 1997), were recognized in front of the epiphysis (Fig. 3A). The epiphysis was strongly immunoreactive to HNK-1, and was associated with a nerve tract, the tract of habenular commissure, which was also HNK-1-positive (Fig. 3A, 4C, also see Figs. 6 and 8 in later stages). The telencephalon was not clearly distinguished from the rest of the forebrain. The anterior tip of the notochord had already emerged at a level slightly caudal to the plica encephali ventralis (Figs. 2B, 3A).

Putative crest cell populations were attached to discrete positions on the dorsolateral aspect of the hindbrain (Fig. 4A). Although rhombomeres were not clearly seen on the surface of the hindbrain, the arrangement of the neuroepithelial cells showed typical neuromeric morphology. In the middle of each rhombomere, neuroepithelial cells were arranged in a fan-shaped pattern and their nuclei located more basally within the epithelium than those in the boundary region (Fig. 3A). Segmental boundaries of rhombomeres were thus identified and the second and third crest cell populations were found associated with rhombomere 4 (r4) and r6, respectively.

The most rostral crest cells had mostly differentiated into the trigeminal nerve anlage containing HNK-1-positive neurons (Fig. 4C). The trigeminal ganglion and (presumably) sensory ganglia of other branchiomeric nerves seemed to contain crest-derived neurons. The trigeminal ganglion grew two branches: a rostral branch that sent fine rami covering the forebrain and optic regions, and a ventral branch that grew and ramified ventrally into the wall covering the yolk sac, beyond the future mandibular arch (Fig. 3B, see below). These branches corresponded to maxillary and mandibular branches of later stages (see below). The trigeminal nerve grew from putative r2, the most expanded region of the hindbrain.

All the embryos at this stage possessed the profundal nerve and ganglion in the cavum epiptericum (the space ventrolateral to the plica encephali ventralis), similar to other Osteichthyes embryos and larvae (Landacre, 1912). Although the position of the ganglion in the cavum appears to be a peculiar one, a similar topography has been illustrated in the earliest profundal nerve anlage of several vertebrates, including amniotes (Stone, 1922; Adelmann, 1925; Kuratani and Tanaka, 1990). Equivalent nerves of the lamprey and shark do not show such topography (Goette, 1914; Kuratani *et al.*, 1997; Kuratani and Horigome, 2000). The Bester profundal ganglion at this stage was still in contact with the epidermal placode, indicating active contribution of the placode to ganglion cells (Fig. 3B, 4H; see below). Proximally, this nerve did not contact the trigeminal nerve, but had an independent root on the hindbrain rostral to the trigeminal nerve root (see below). Neurites from other cranial sensory ganglia had also grown centrally to merge into the dorsolateral fasciculus (Fig. 4C, D).

Caudal to the trigeminal nerve, acusticofacial and glossopharyngeal nerves had formed. The primordia of geniculate and petrosal ganglia contacted the focal thickenings of the surface ectoderm at the levels of the first and second pharyngeal pouches, indicating the contribution of epibranchial placodes to these ganglia (Fig. 3B). From the geniculate gan-

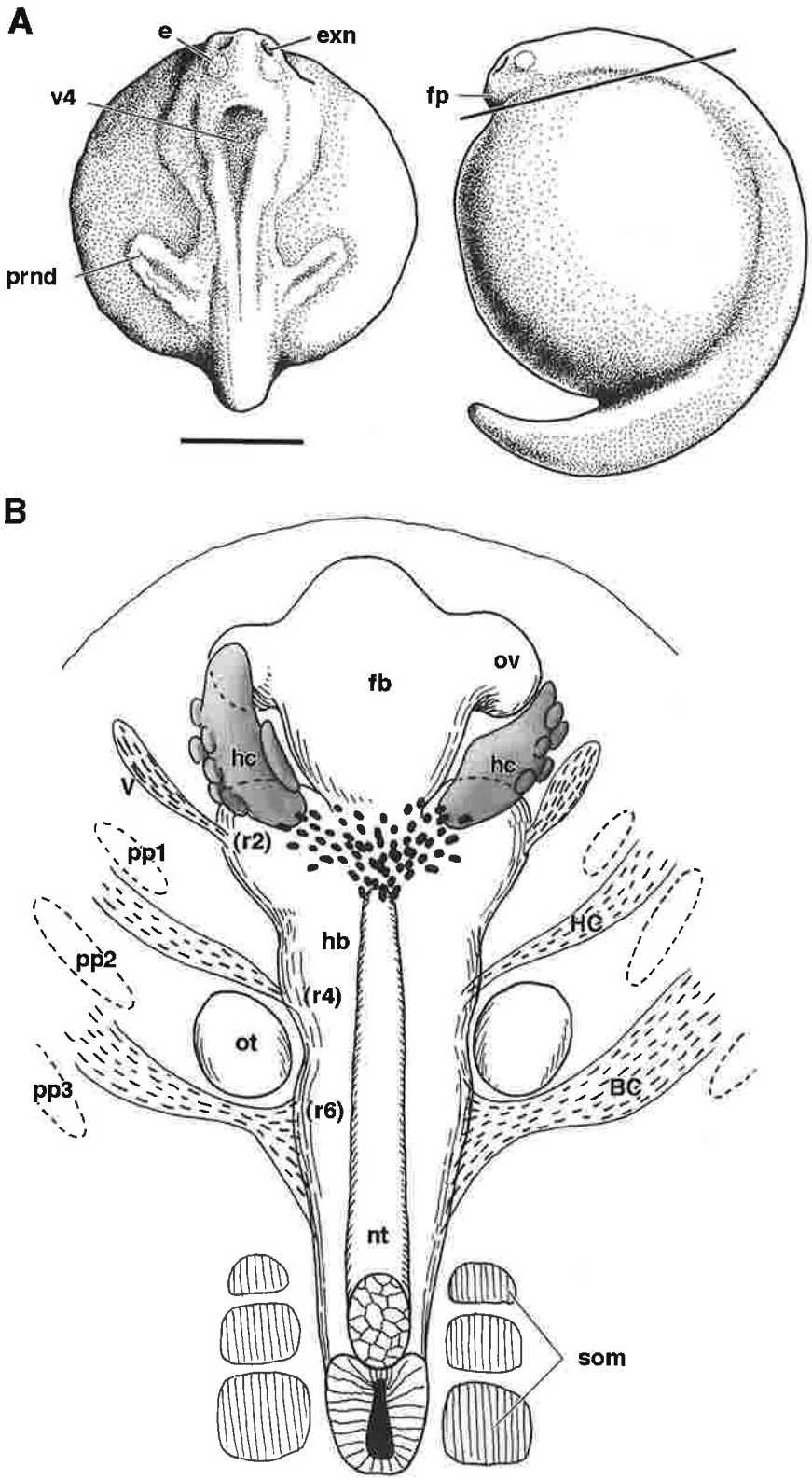

Fig. 2. Stage A embryos of Bester. **A**: External morphology of the embryo. Dorsal (left) and lateral (right) views. The line indicates the plane from which the reconstruction was viewed in B. **B**: Ventral view of the reconstructed embryo. Three cephalic crest cell populations (V, HC, BC) extend from the hindbrain and are peripherally distributed in each pharyngeal arch. Of those, the most rostral cell population has differentiated into the trigeminal nerve ganglion (V). Beneath the optic vesicle (ov), a pair of mesodermal epithelia, or head cavities (hc) has developed. The basal surface of the cavity is rough and is associated with small protrusions or independent epithelial cysts. Note that a dense mesodermal mesenchyme is present, connecting the pair of head cavities and the rostral tip of the notochord (nt). Bar = 1 mm.

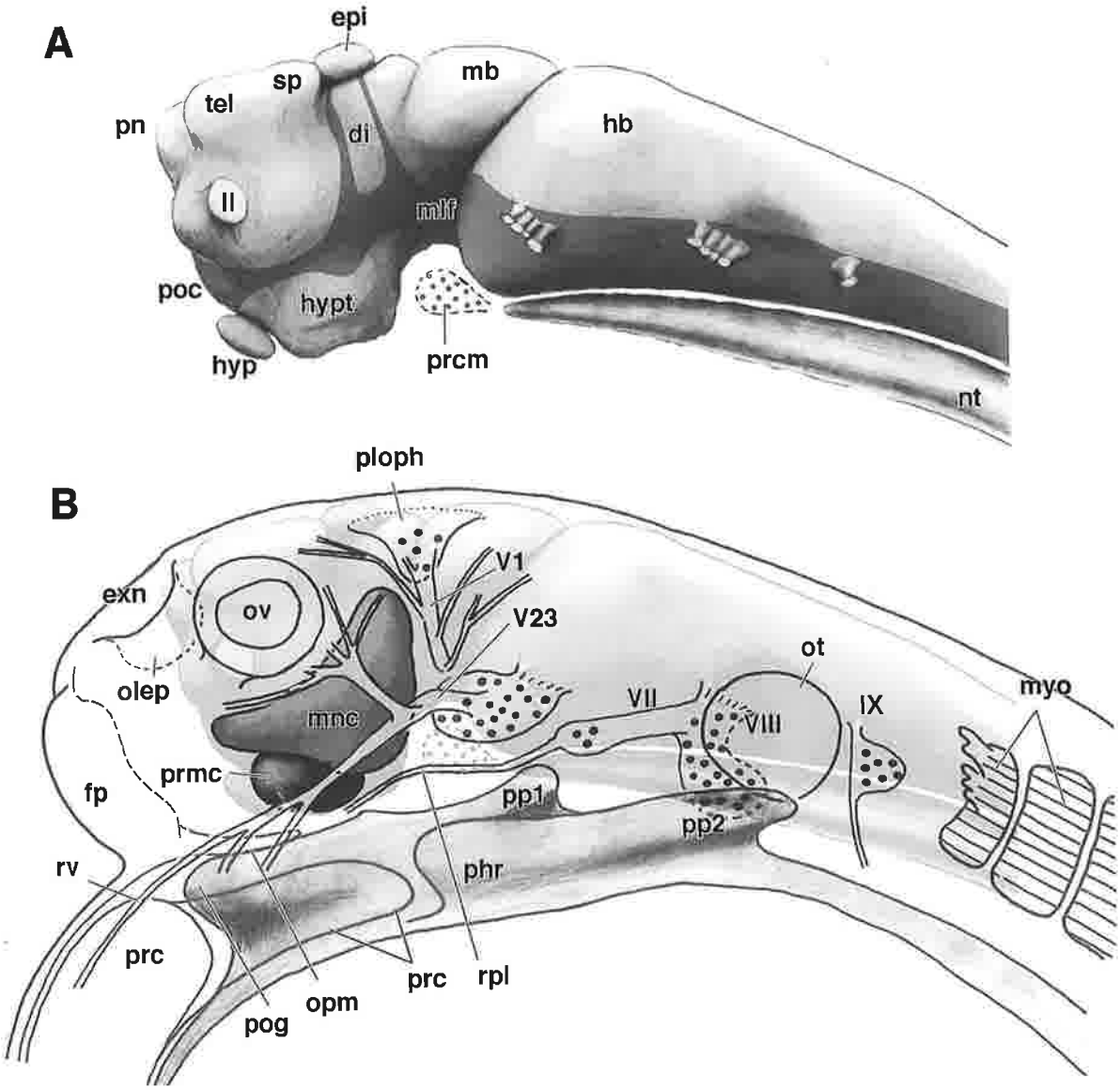

Fig. 3. Graphic reconstruction of a stage A embryo. Lateral views. **A**: External morphology of the brain. The developing nerve tracts are shaded. Note the prechordal mesenchyme (prcm) beneath the plica encephali ventralis. **B**: Reconstructed embryonic structures are superimposed on the brain. Peripheral nerve ganglia are stippled. This embryo is slightly older than that illustrated in Fig. 2B. The head cavity has been incompletely separated into two components, the medial, or the premandibular cavity (prmc), and the more laterally located mandibular cavity (mnc). Note that the mandibular cavity is inserted between profundal (V1) and trigeminal (V23) nerves.

glion, a branch grew rostrally for a long distance into the future upper jaw region, representing the palatine branch of the facial nerve that innervates barbels at later stages. All the branchiomeric nerve roots were proximally connected to the dorsolateral fasciculus. The latter tract contained fibers from the above-noted sensory ganglia and Rohon-Beard cells in the caudal part of the hindbrain and the spinal cord (Fig. 4C to E).

Rostral to the anterior tip of the notochord, beneath the cephalic flexure, was a dense mesenchyme that expanded rostrolaterally to attach to a pair of mesodermal epithelial structures, the head cavities, on both sides of the diencephalon and beneath the optic vesicle (Fig. 2B). The cavities were spindle-shaped, with a number of small cysts and epithelial processes on the surface (Fig. 2B). In slightly older embryos, the cavities began to be divided into a small and ventrally located cavity, and a dorsally located larger cavity on each side (Fig. 3B). The latter was located between the ophthalmic profundus nerve and the maxillomandibular nerve (Figs. 3B, 4H, I). From the position and morphology, this cavity corresponded to the mandibular cavity of the shark embryo (Galeus canis: van Wijhe, 1882; 4.5-mm *Squalus acanthias*: de Beer, 1922; *Scyliorhinus torazame*: Kuratani and Horigome, 2000), and the smaller one to the premandibular cavity (Kuratani and Horigome, 2000; and refs. therein). These cavities were not separated completely from each other (Fig. 4F to I). In no

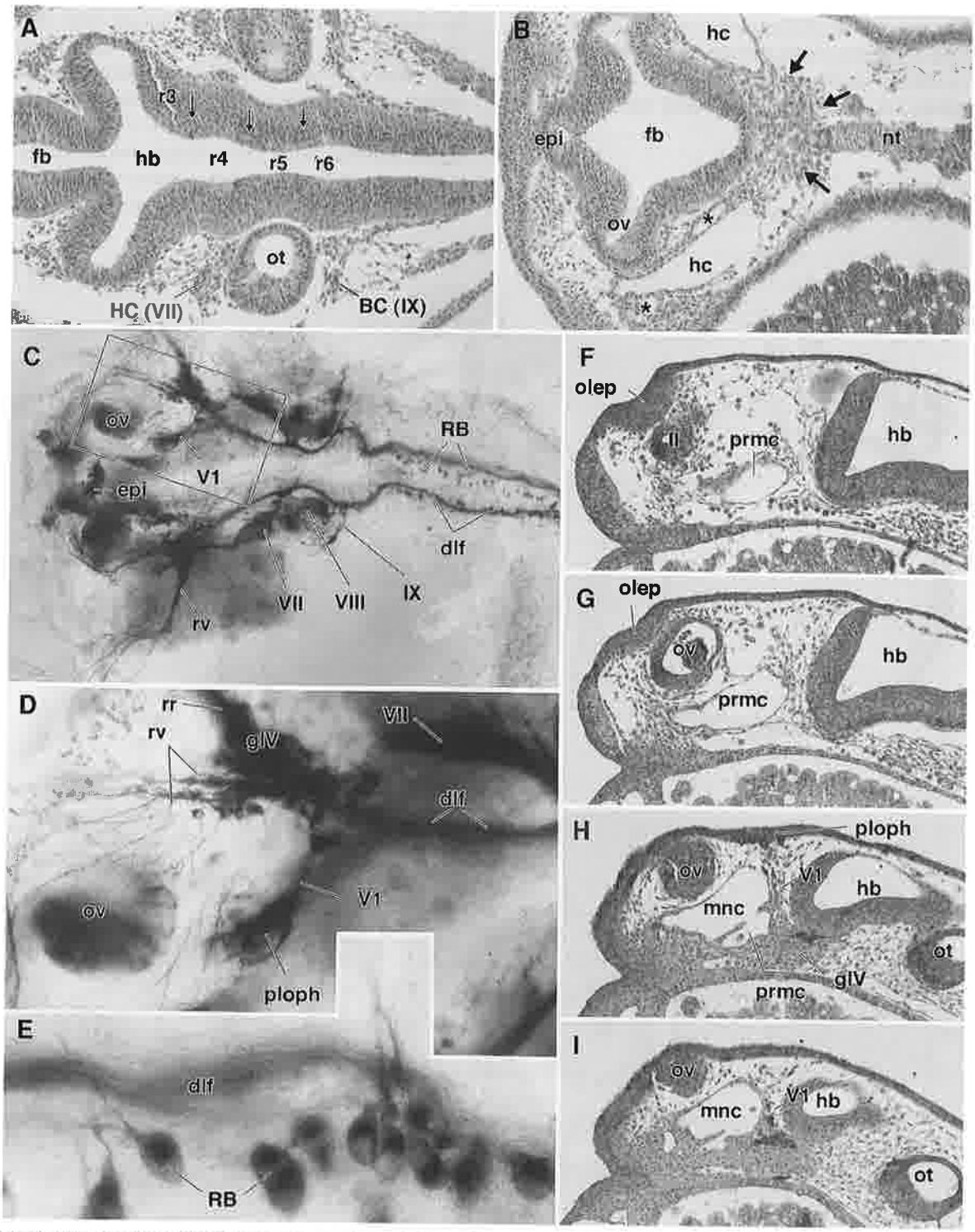

Fig. 4. Histological and immunohistological observations of stage A embryos. **A**: Horizontal section through the anteroposterior axis of the rostral hindbrain. Development of rhombomeric compartments is apparent by neuroepithelial arrangement (rhombomeric boundary levels indicated by arrows). At levels of r2 and r4, putative cephalic crest cell populations (HC, BC) are attached to the meningeal surface of the hindbrain representing facial and glossopharyngeal nerve primordia, respectively. **B**: Another horizontal section from the same embryo as in A, cut through the notochord (nt) and head cavities (hc). Note the dense prechordal mesenchyme distributed between the cavities on both sides and the rostral tip of the notochord (arrows). Asterisks indicate small epithelial cysts associated with the head cavity. **C**: A whole-mount embryo immunochemically stained with HNK-1, seen from the dorsal view. Developing nervous system is stained. **D**: Enlargement of the box in C.[OLE12] Fine neurites are developing from placodal cells. **E**: Enlargement of Rohon-Beard cells in the caudal hindbrain level of the same embryo as shown in C. Neurites of Rohon-Beard cells contribute to the formation of the dorsolateral fasciculus (dlf) or grows laterally into the trunk epidermis. **F–I**: HNK-1-stained histological sections from the same embryo as shown in Fig. 3, which have been cut parasagittally. Sections are arranged in order from medial to lateral levels. Note that premandibular and mandibular cavities are not entirely separated from each other (H).

embryo was the premandibular cavity found in contact with the rostral tip of the notochord, indicating that the mandibular and premandibular cavities arose as a single epithelial cyst simultaneously. No mesodermal epithelial cyst was found caudal to these cavities.

Stage B

Bester embryos hatch between stages A and B (table 1). By stage B, the head cavity had not yet been divided completely (Fig. 5D). The division of the cavities was distinct rostrally, where the two subdivisions showed certain histological differences. Thus, the premandibular portion of the cavity consisted of thicker epithelial cells than that of the mandibular subdivision (Fig. 5C). Furthermore, the lateral cavity was ventrally attached to a dense mesenchyme within the mandibular arch, representing the mandibular arch muscle plate (Fig. 5C,

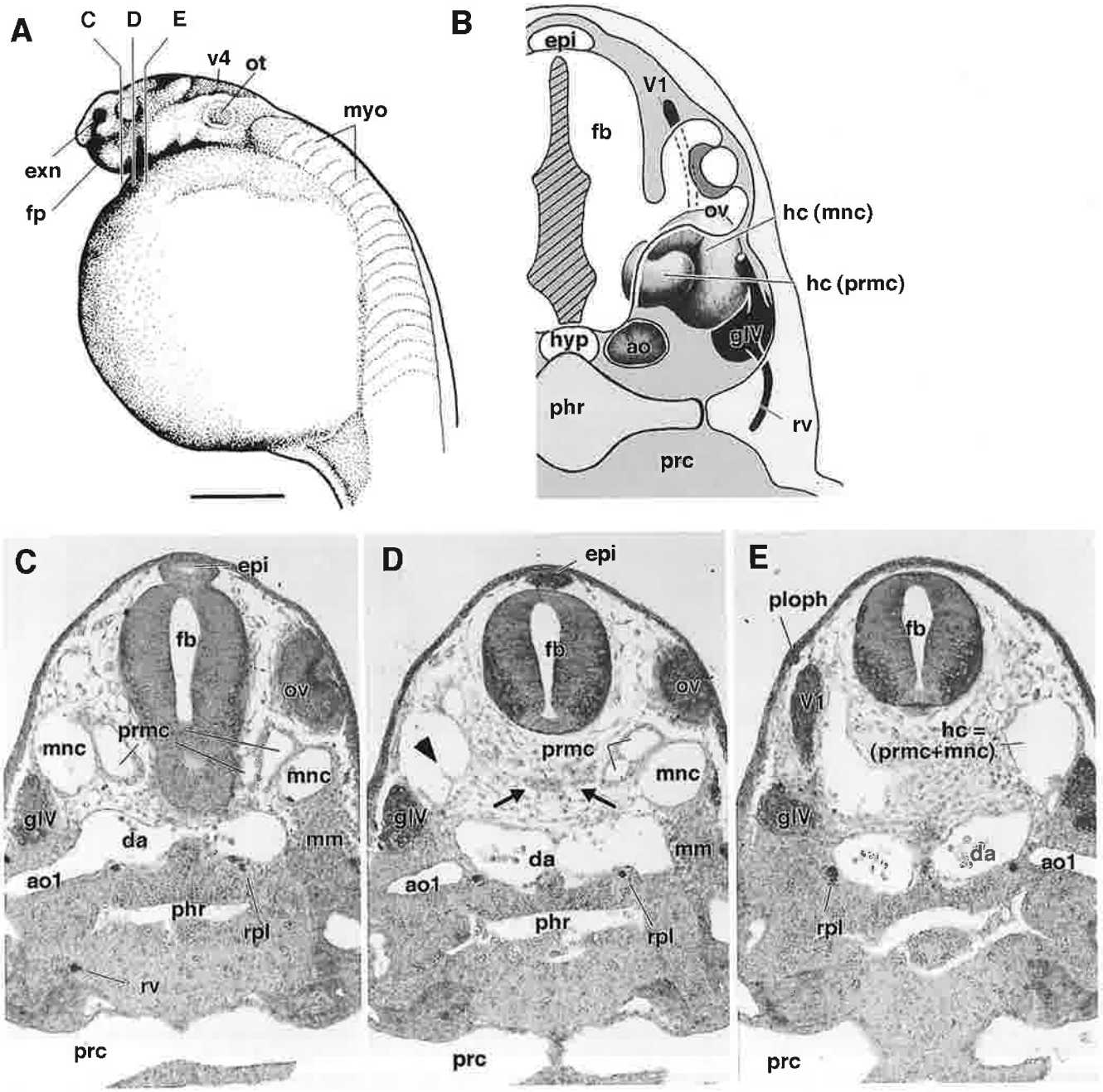

Fig. 5. Stage B embryo. **A**: External morphology of the stage **B** embryo. B: Graphical reconstruction of the head cavity based on transverse sections shown in C to D. Note that the head cavity is mediolaterally subdivided into the premandibular and mandibular cavities. **C–E**: Transverse sections stained immunochemically with the HNK-1 antibody. Note that the division of the head cavities is distinct anteriorly (C), but incomplete caudally (E). Arrowhead in D indicates an indentation in the cavity wall. Arrows in D indicate the premandibular mesenchyme that spans the premandibular cavities on both sides.

D). A similar topographical relationship has been described in elasmobranch (Bjerring, 1977; Kuratani and Horigome, 2000) and lamprey embryos (Kuratani *et al.*, 1999), consistently indicating the homology of this cavity.

In the peripheral nervous system at stage B, the neurite network in the epidermis had developed more extensively in both the head and trunk regions than at stage A (Fig. 6A). In the head, some of the neurites originated from the HNK-1-positive placodal cells scattered in the trigeminal domain (including the profundal region), and many others could be traced to the trigeminal and ophthalmic ganglia. Thus, the contribution from the epidermal placodes was apparent, not only for the profundal, but also for the trigeminal ganglion. Such a scattered distribution pattern of placodes has been observed in the trigeminal domain of various vertebrate embryos (van Campenhout, 1936; Batten, 1957 a, b; Kuratani and Hirano, 1990), which stands in contrast to the so-called epibranchial placodes associated with other branchiomeric nerves (see below).

The profundal nerve still possessed its own nerve root, rostral to the trigeminal nerve root (Fig. 6B). Although the r1/2 boundary was not clear, the close relationship between trigeminal and profundal nerve roots indicates that both issued from r2 (Fig. 6B). The anterior lateral line ganglion first appeared with its own nerve root that connected to the dorsolateral fasciculus at a level slightly caudal to the facial nerve root, and rostral to the acoustic nerve root (Fig. 6A, B). From the facial nerve, the palatine branch grew rostrally beneath the dorsal aorta to a region dorsolateral to the frontal process, where the nerve bifurcated and formed a brush of numerous nerve fibers together with fibers from the rostral branch of the trigeminal nerve (Figs. 5C to E, 6A). Barbel primordia later grew from this place (see below). Since the barbels develop in the maxillary processes of larvae, this trigeminal nerve branch would correspond to the maxillary branch in other vertebrates. In many vertebrate species, the maxillary branch (often called the infraoptic nerve) and palatine branch of the facial nerve form anastomoses in a similar region, where they are involved in the sensory function of the skin (reviewed by Hallerstein, 1933).

Stage C

In stage C, pharyngeal arches 2 and 3 could be distinguished. The position of the second pharyngeal groove corresponded approximately to the level of the otocyst. Beneath the eye and dorsal to the frontal process, there was a swelling on the surface of the larva, indicating the initial development of the barbel (Fig. 6C).

The maxillomandibular prominence became visible on the surface at this stage. The epidermal neurites had diminished as compared with stage B (Fig. 6D, cf. Fig. 6A). An interesting change was recognized in the profundal nerve ganglion, where a new connection had been established with the trigeminal ganglion (Fig. 6D). At this stage and at stage B, epidermal cells showed local staining with HNK-1 antibody, corresponding to the epibranchial placodes. Since the undifferentiated dorsolateral placode was never stained with the same antibody (see below), HNK-1 can be regarded as a reliable marker of epibranchial placodes. As observed in histological sections, however, the placodal contributions to the branchiomeric sensory ganglia were already apparent at stage A (Fig. 3B).

In addition to the palatine branch, the facial nerve at this stage possessed another branch-the post-trematic branch that grew ventrally into the second pharyngeal arch (Fig. 6D).

Stage D

The pectoral fin bud was first observed at this stage. In the head, the maxillomandibular prominence and primordia of the barbels were clearly distinguished on the surface (Fig. 7B). The latter consisted of two pairs of prominences mediolaterally arranged on the future maxillary region (not shown). The dorsal root ganglion was also observed as an HNK-1-positive cell mass in the postotic region (Fig. 7A).

In the cranial nerve, all the epibranchial placodes (geniculate, petrosal and nodose placodes) had appeared on the epidermis as HNK-1-immunoreactive regions dorsolateral to the pharyngeal pouches (Fig. 7A). In the histological section, these placodes were seen as local epidermal thickenings that were in contact with the sensory ganglion primordia of branchiomeric nerves medially (not shown), indicating an active contribution of neuroblasts to these ganglia. From these epibranchial ganglion-placode complexes, as a rule, post-trematic branches grew ventrally into each pharyngeal pouch. That of the facial nerve issued a superficial ramus that also passed ventrally. The rest of the branch was located in a deeper part of the arch, representing the hyomandibular nerve. Distally, it further bifurcated mediolaterally into two ramules, of which the medial branch probably represents the earliest development of the internal mandibular branch or the chorda tympani. The lateral component of the post-trematic branch was the opercular branch.

No pre-trematic branches were apparent in branchiomeric nerves. In addition to the pharyngeal branches, the facial and glossopharyngeal nerves possessed dorsally-growing pharyngeal branches; of these, that of the facial nerve was the palatine nerve, and that of the glossopharyngeal was the dorsal pharyngeal branch (Fig. 7A). Thus, the branchiomeric nerve exhibited typical metameric morphology at this stage.

The most conspicuous change that had occurred by this stage was seen in the profundal nerve. Thus, the nerve had totally lost its own nerve root on the hindbrain (see Fig. 6A, D), and was now connected proximally only to the trigeminal ganglion (Fig. 7A, C). Although the epidermal neurite network had further diminished, the portion that covered the fore-midbrain to the ocular region remained in association with the ophthalmic placode cells. These neurites were connected to the profundal nerve as before.

The lateral line nervous system consisted of components of the anterior lateral line nerve, namely, the superficial ophthalmic and buccal branches as well as the anterior lateral line ganglion, and one middle lateral line nerve component that developed independently at the level of the glossopha-

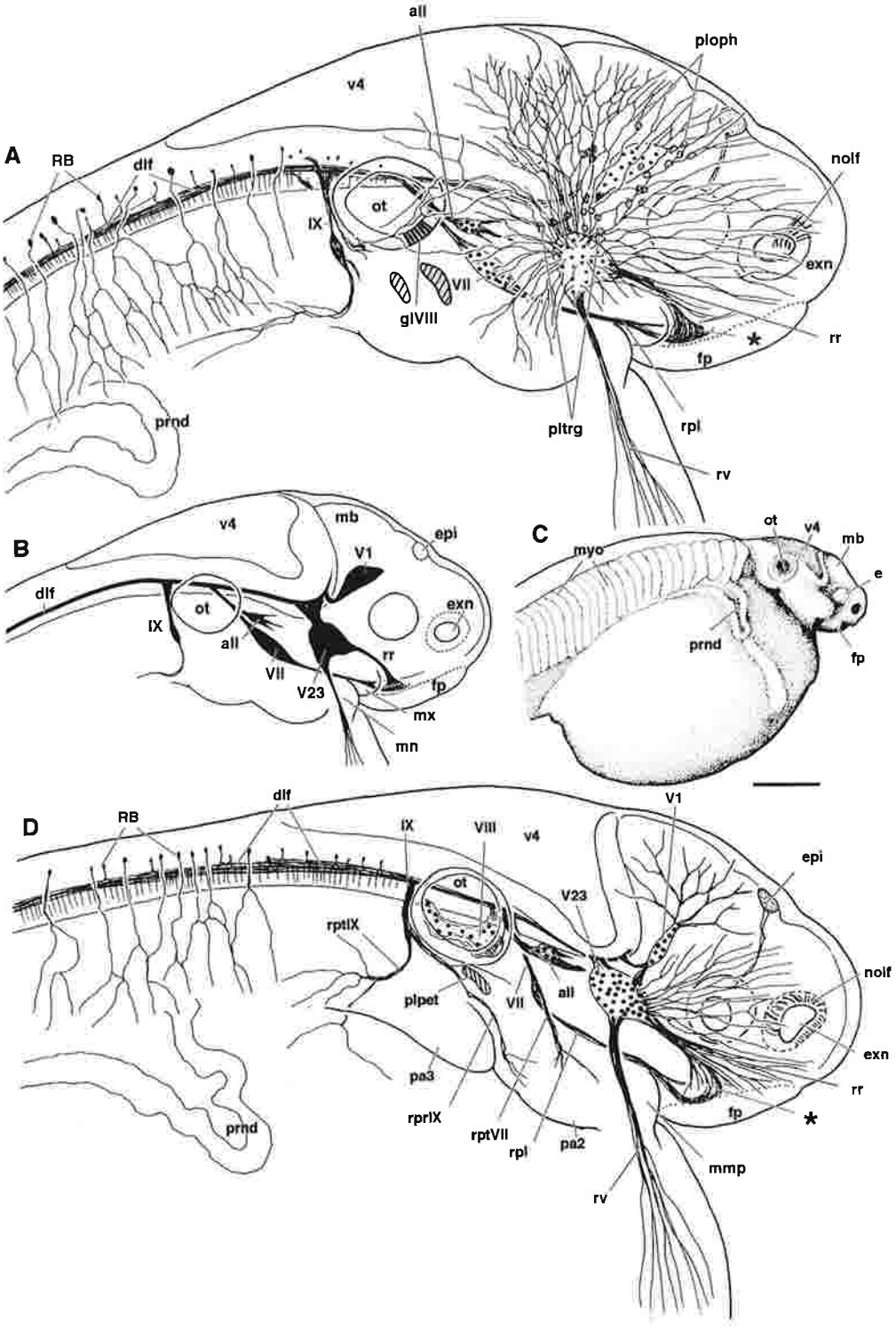

Fig. 6. Peripheral nerve development at stages B and C. **A**: Illustration of a stage B embryo immunochemically stained with HNK-1. Putative sensory ganglia are stippled. Extensive and poorly organized distribution of fine neurites is recognized within the epidermis of the embryo. In the head, the neurites appear to originate from placodal cells (cells labeled "ploph" and "pltrg"), that are also HNK-1-positive and scattered within the epidermis over the trigeminal domain, and those in the trunk from the Rohon-Beard cells (RB). Asterisk (also in D) indicates the nerve network developing in the future barbel. **B**: Schematic illustration of the same embryo as in A. Note that the profundal nerve possesses its independent nerve root on the hindbrain. **C**: External morphology of the Bester embryo at stage C. **D**: Peripheral nerve morphology. Superficial neurites have decreased in number as compared to stage B embryo. Note that the mandibular nerve extends neurites within the epidermis covering the pericardium, far beyond the domain of the mandibular process (mn). Also, note that the profundal nerve (V1) has now established a connection with the trigeminal ganglion (V23). The only lateral line component at these stages is the primordium of the anterior lateral line nerve (all), the nerve root of which has developed slightly rostral to that of the facial nerve (VII). Bar in C=1 mm.

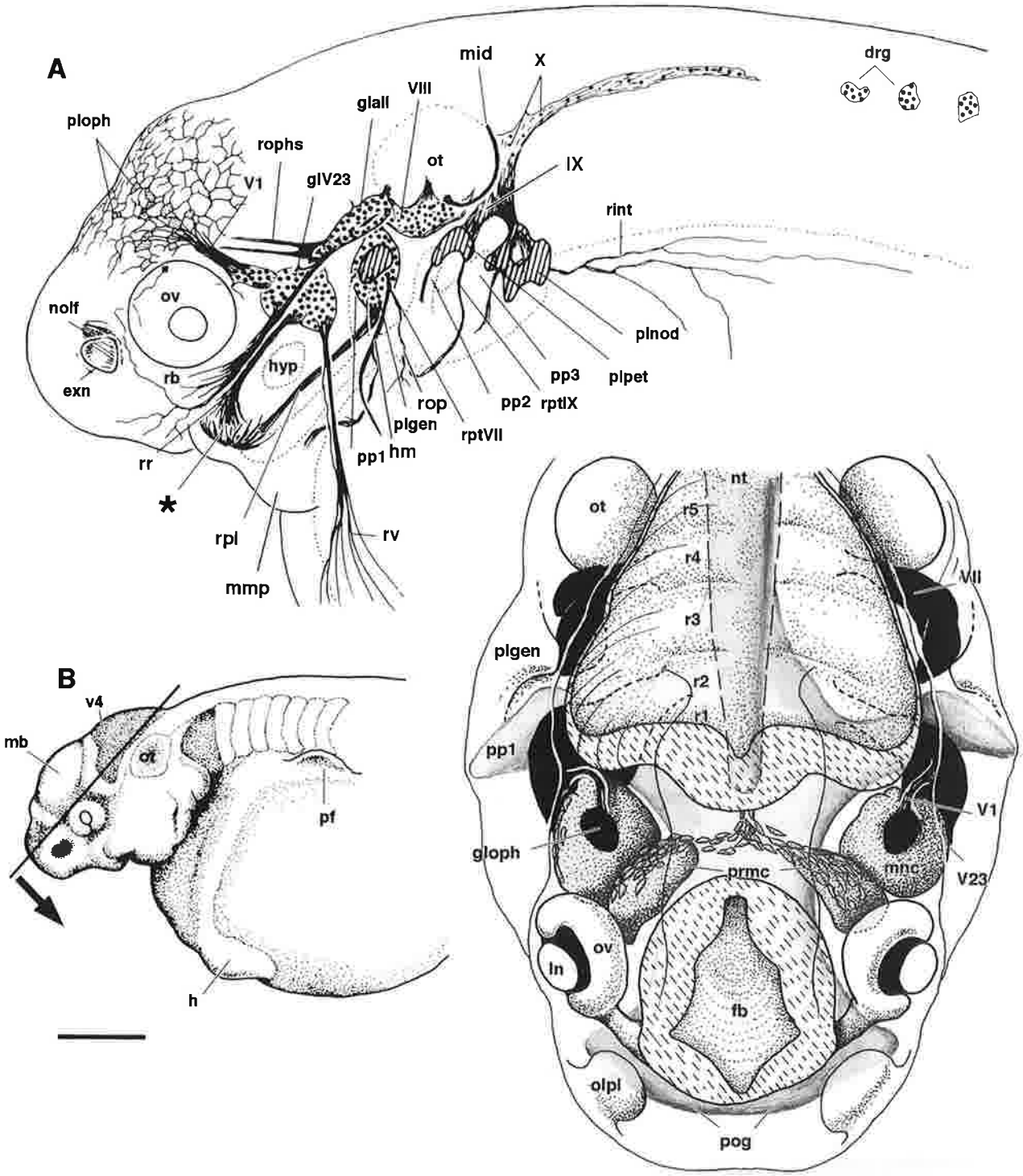

Fig. 7. Stage D embryos. **A**: Peripheral nerve morphology is illustrated based on an HNK-1-immunostained whole-mount specimen. All the placodes have appeared as HNK-1-positive epidermal portions (shaded). Metameric arrangement of branchiomeric nerves is apparent. Most of the immunoreactive neurites have been fasciculated into solid nerve branches. Dorsal root ganglia (drg) are first visible. The superficial neurites have reduced in number, though not entirely disappeared. The Rohon-Beard neurites have also reduced in the trunk, consisting of very fine fibers, which are not illustrated here. Barbel anlage is protruding (asterisk) and receiving numerous nerve processes derived from both trigeminal and facial nerves. Note that the profundal nerve root has disappeared and the nerve has now appeared as a branch of the trigeminal nerve. **B**: External morphology of a stage D embryo. **C**: Graphic reconstruction of a stage D embryo based on histological serial sections. The model is seen from the dorsoanterior view indicated by a line and an arrow in B. Note that the mandibular cavity is situated between the same profundal and trigeminal nerves as stage A (Fig. 3), and that trigeminal and facial nerve roots are located on r2 and r4, respectively. Bar in B=1 mm.